Contribution ID: **887** Type: **Regular Poster**

ITER baseline scenario investigations on TCV and comparison with AUG

Wednesday, 12 May 2021 18:25 (20 minutes)

Under the auspices of EUROfusion, the ITER baseline scenario (IBL, [1]) is jointly investigated on AUG and TCV. While AUG results were presented at the last IAEA [2], this contribution focuses on recent results obtained in TCV. Such developments in TCV were only possible with the installation of an NBI heating source [3], allowing ELMy H-modes at ITER relevant β_N. The IBL scenario is mainly characterized by low q_{95} (3-3.6), high positive triangularity (δ>0.3) and relatively high elongation (κ>1.6). In AUG, these combinations lead to very steep and narrow edge transport barriers, when good confinement is obtained, with high pedestal pressure and therefore large Type-I ELM crashes. A similar behavior is also observed on TCV, since indeed the target plasma shape has been derived from the IBL AUG shape, as shown in Fig. 1.

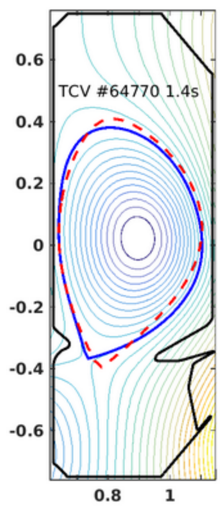

Figure 1: TCV shape (blue) with AUG IBL (dashed) rescaled

The AUG shape (dashed red) has been rescaled to match TCV geometrical radius and further rescaled to match the minor radius, since there is a 20% difference in aspect ratio. As can be seen from Fig. 2, the TCV triangularity is slightly increased as compared with AUG, in order to approach the ITER design one, while the elongation is slightly smaller. It should be emphasized that a positive triangularity of 0.3-0.5 falls exactly in the steepest region regarding the sensitivity of the pedestal pressure versus (averaged) triangularity ([4], Fig. 10).

	AUG	TCV	ITER
delta top	0.25	0.29	0.49
delta bottom	0.40	0.55	0.50
delta average	0.33	0.42	0.50
kappa	1.73	1.65	1.84

Figure 2: Top, bottom and average triangularities and elongation in IBL scenarios at AUG, TCV and scenario 2 of ITER

The global performance of the recent TCV IBL discharges is reported in the usual diagrams of H_{98y2} vs β_N, as well as AUG results [2] (Fig. 3). Fig. 3a shows that ITER target values (β_N=1.8 and H_{98y2}=1, q_{95}˜3-3.2) have been obtained, similarly to AUG (Fig. 3b). On AUG, a scenario with q_{95}˜3.6, β_N=2.2 and H_{98y2}=1.2, to keep $\beta_N H_{98y2}/(q_{95})^2$ constant has been further studied as well.

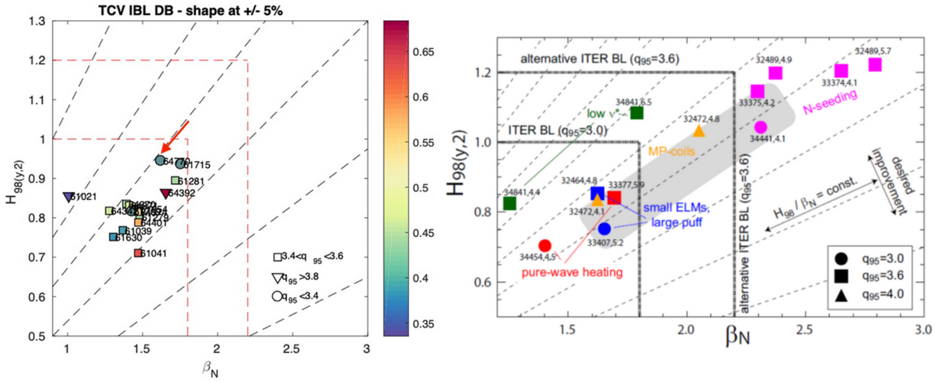

Figure 3: (a) H_{98y2} factor vs β_N at the time just before a large ELM crash for recent TCV ITER baseline scenario heated with NBI mainly and X3 in some cases. (b) AUG recent results with grey area representing previous results [2].

Currently such scenario has not been tried on TCV at maximum power, the developments at lower current (β_N<1.7) being focused on stationary discharges without MHD modes (Fig. 3a). The time traces of the discharge 64770, highlighted with a red arrow in Fig. 3(a), are shown in Fig. 4 (red). The various phases are representative of the studies that will be discussed in this work. The high current (275kA, q_{95}=3.2) phase starts at 1.3s and lasts about 150ms (dashed lines) with β_N˜1.6 before a 3/2 mode is triggered at the 3rd ELM crash yielding β_N˜1.3-1.4 and a 2/1 mode at 1.5s leading to β_N<1 at which value it self-stabilizes. The confinement time is about 35ms (H_{98y2}=0.95), the ELM period 50-65ms (15-20Hz) and the current redistribution time 100-150ms. The "stationary" time interval marked in Fig. 4 by the dashed lines is therefore about one current redistribution time, which is quite long and comparable to other tokamaks IBL scenarios, however only 4-5 energy confinement times and only 3 ELM periods. The high triangularity and TCV short current redistribution time may lead to significant magnetic perturbation at ELM crashes which tend to systematically trigger low m/n modes, sometimes directly a 2/1 mode eventually locking but not necessarily leading to a disruption (as in 64678, Fig. 4black). This will be compared to the relation between sawtooth period, resistive time and NTM onset shown in Ref. [5]. The sensitivity to NTM onset explains why the developments of the TCV IBL largely rely, at first, in the establishment of a stationary phase at q_{95}>4 and then the discharge can evolve towards q_{95}=3.6 or 3-3.2 for studying both IBL scenarios already achieved on AUG [2]. Initiating the H-mode phase at reduced I_p has another advantage which is to avoid any problem with the L-H transition and potentially large 1^{st} ELM. This was already observed related to NTMs triggered by the first long sawtooth period when entering in H-mode on JET. All these transient events are much better controlled when occurring at q_{95}>4.5, including the transition into H-mode and the final shape development. This is in a large part also used in the AUG IBL scenario.
The important role of 3^{rd} harmonic (X3) ECH in preventing low m/n MHD modes onset in TCV is reported. This has been clearly demonstrated in TCV, but up to a maximum plasma current so far (Ip=240kA) corresponding to q_{95}=3.6-4. This is also seen in Fig. 4, where the first phase at lower plasma current has a nice stationary ELMy H-mode with no significant MHD activity, contrary to a similar shot without X3 (64678). Note that the latter has a 2/1 mode stabilizing and the discharge recovers to high β_N values (1.5-1.6s). The possible reasons for this plasma current/q_{95} dependence on MHD activity prevention will be analysed. On the one hand, it is more difficult to influence the global q profile with electron heating at high total plasma current, on the other hand higher I_p leads to higher density on TCV (relatively open divertor and no pumping). For example, in #64770, X3 absorption is around 15-20% in the first phase, 0.8-1.2s (Fig. 4) but reduces to less than 5% at the maximum current when the line-averaged density reaches 1.1e20 m^{-3}. Since significant density peaking is observed in these discharges, the central density reaches values above 1.6e20 m^{-3}, the cut-off density of the X3 heating sources. The density peaking itself can lead to a stronger electron temperature flattening and to plasmas more prone to instabilities. Gyrokinetic studies and density peaking predicted by quasi-linear analyses will be presented.

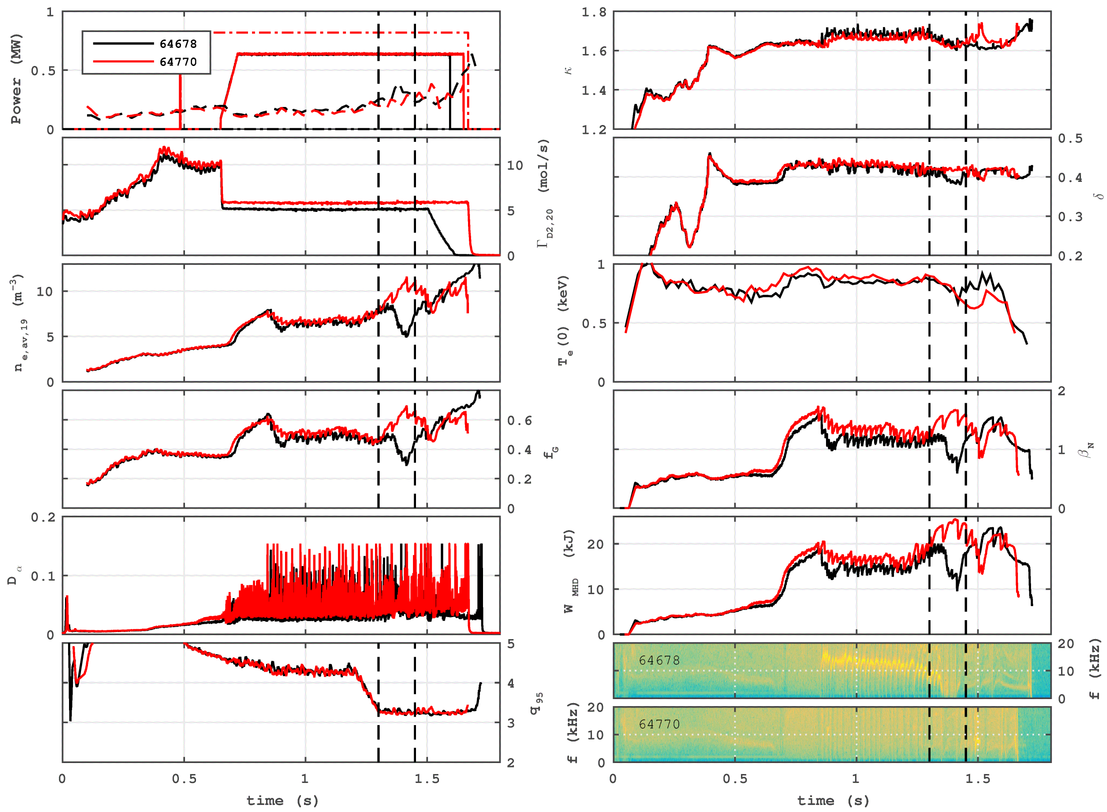

Figure 4: TCV time traces with the interval 1.30s-1.45s marked with dashed lines at q_{95}=3.2 and without significant MHD (for 64770 with X3). This corresponds to about 4-5 confinement times and one current redistribution time.

It is worth mentioning that no significant carbon accumulation has been observed so far, however dedicated impurity seeding experiments have to be performed. The role of ECH versus NBI heating will be discussed, in particular at lower plasma current where X3 is still absorbed and with regards to the effects on density peaking. The latter might be due to improved core confinement. In most TCV IBL cases $T_e\tilde{}T_i$ due to the relatively high density. Note that the Greenwald fraction obtained on TCV is still below about 0.6 despite the new baffles, while AUG obtains discharges up to Greenwald densities.

In AUG, recent discharges comparing heating mix, pellets vs gas puff and nitrogen seeding essentially provided similar performances as previously observed (grey area in Fig. 3b). Only the lower collisionality cases seem to recover the ITER design performance (green points). These low density discharges rely on magnetic perturbation and are quite difficult to obtain without locked mode.

Finally, controlled ramp-down phases, including safe H-L exit, were tested with the IBL scenario on AUG, guided by simulations [6], and reproducible, safe and relatively fast ramp-down have been obtained, showing how a combined control of current ramp-rate, shape and power can be beneficial.

References

[1] A. C. C. Sips et al, Nucl. Fusion **58** (2018) 126010

[2] T. Pütterich et al, 2018 IAEA FEC, IAEA-CN-EX/P8-4

[3] A. Fasoli et al, Nucl. Fusion **49** (2009) 104005

[4] A. Merle et al, Plasma Phys. Control. Fusion **59** (2017) 104001

[5] I. T. Chapman et al, Nucl. Fusion **50** (2010) 102001

[6] A. A. Teplukhina, Plasma Phys. Control. Fusion **59** (2017) 124004

Affiliation

Ecole Polytechnique Fédérale de Lausanne (EPFL), Swiss Plasma Center (SPC), CH-1015 Lausanne, Switzerland

Country or International Organization

Switzerland

Primary authors: SAUTER, Olivier; PÜTTERICH, Thomas (Max-Planck-Institut für Plasmaphysik); BAGNATO, P. (SPC-EPFL); BOBKOV, Volodymyr (Max-Planck-Institute for Plasma Physics); CAMENEN, Yann (CNRS); CODA, Stefano (CRPP-EPFL); DUNNE, Mike (IPP-Garching); Dr ERIKSSON, F. (Chalmers University of Technology); FRANSSON, E. (Chalmers University of Technology); Dr KARPUSHOV, A. (SPC-EPFL); LABIT, BENOIT (Swiss Plasma Center (SPC) EPFL SWITZERLAND); LANG, Peter (Max-Planck-Institut fűr Plasmaphysik); MANTSINEN, Mervi (ICREA and Barcelona Supercomputing Center); Dr MARASCHEK, Marc (IPP-Garching); MCDERMOTT, Rachael (Max Planck Institut für Plasmaphysik); MERLE, Antoine (Ecole Polytechnique Fédérale de Lausanne (EPFL), Centre de Recherches en Physique des Plasmas (CRPP), CH-1015 Lausanne, Switzerland); NEUBERT, Ph. (IPP-Garching); STOBER, Joerg (IPP Garching); SUTTROP, Wolfgang (Max-Planck-Institut für Plasmaphysik); Dr VALLAR, M. (SPC-EPFL); VOITSEKHOVITCH, Irina (CCFE); WIDMER, Fabien (Aix-Marseille University); WILLENSDORFER, Matthias (IPP Garching); TCV TEAM (Ecole Polytechnique Fédérale de Lausanne –Swiss Plasma Center (SPC), Association Euratom-Confédération Suisse(EPFL) CH-1015 Lausanne, Switzerland); ASDEX UPGRADE TEAM (arne.kallenbach@ipp.mpg.de); EUROFUSION MST1 TEAM

Presenter: SAUTER, Olivier

Session Classification: P4 Posters 4

Track Classification: Magnetic Fusion Experiments